

TRIANGULAR SPHERICAL DIHEDRAL F-TILINGS: THE $(\pi/2, \pi/3, \pi/4)$ AND $(2\pi/3, \pi/4, \pi/4)$ FAMILY

CATARINA P. AVELINO AND ALTINO F. SANTOS

ABSTRACT. We classify all the dihedral f-tilings with spherical triangles $(\frac{\pi}{2}, \frac{\pi}{3}, \frac{\pi}{4})$ and $(\frac{2\pi}{3}, \frac{\pi}{4}, \frac{\pi}{4})$, and give the combinatorial structure, including the symmetry group of each tiling.

1. INTRODUCTION

Let S^2 be the sphere of radius 1. By a *folding tiling* (*f-tiling*, for short) of the sphere S^2 we mean an edge-to-edge finite polygonal tiling τ of S^2 such that all vertices of τ satisfy the *angle-folding relation*, i.e., each vertex of τ is of even valency and the sums of alternating angles around each vertex are equal to π .

Folding tilings are intrinsically related to the theory of isometric foldings of Riemannian manifolds, introduced by S. A. Robertson in 1977 [8]. In fact, the edge-complex associated to a spherical f-tiling is the set of singularities of some spherical isometric folding.

A spherical f-tiling τ is called *monohedral* if every tile of τ is congruent to one fixed set X ; it is called *dihedral* if every tile of τ is congruent to either of two fixed sets X and Y .

The classification of f-tilings was initiated by Ana Breda [2], with a complete classification of all spherical monohedral (triangular) f-tilings. Later on, in 2002, Y. Ueno and Y. Agaoka [9] have established the complete classification of all triangular monohedral tilings of the sphere (without any restrictions on angles).

The study of all dihedral spherical f-tilings whose prototiles are an equilateral triangle and an isosceles triangle was presented in [4]. For a list of all dihedral f-tilings of the sphere by equilateral and scalene triangles see [3]. The study of f-tilings by isosceles triangles and scalene triangles started recently; see [1].

Robert Dawson has also been interested in special classes of spherical tilings; see, for instance, [5, 6, 7].

2010 *Mathematics Subject Classification.* 52C20, 52B05, 20B35.

Key words and phrases. Dihedral spherical f-tiling; Combinatorial properties.

This research was supported by FCT – Fundação para a Ciência e a Tecnologia, through projects UID/MAT/00013/2013 of CMAT-UTAD, Center of Mathematics of University of Minho, and UID/Multi/04621/2019 of CEMAT/IST-ID, Center for Computational and Stochastic Mathematics, Instituto Superior Técnico, University of Lisbon.

In this paper we shall discuss dihedral f-tilings of S^2 with prototiles the spherical triangles

$$T = (\beta, \gamma, \delta) = \left(\frac{\pi}{2}, \frac{\pi}{3}, \frac{\pi}{4}\right) \quad \text{and} \quad T' = \left(\frac{2\pi}{3}, \frac{\pi}{4}, \frac{\pi}{4}\right).$$

Observe that the right triangle T is half of the triangle T' ; this can be seen bisecting T' through the angle $\frac{2\pi}{3}$ (Figure 1).

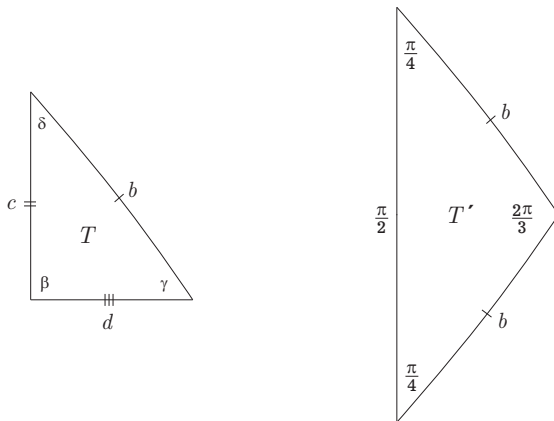


FIGURE 1. The spherical prototiles T and T'

We shall denote by $\Omega(T, T')$ the set, up to an isomorphism, of all dihedral f-tilings of S^2 whose prototiles are T and T' . Using spherical trigonometry formulas, we conclude that the edge lengths of T are

$$b = \arccos \frac{\sqrt{3}}{3}, \quad c = \frac{\pi}{4}, \quad \text{and} \quad d = \arccos \frac{\sqrt{6}}{3}, \quad (b + d = \pi/2).$$

A. Breda proved in [2] that T is the prototile of exactly two spherical f-tilings while there is no monohedral f-tiling with prototile T' . In this paper we show that combining the spherical triangles T and T' we obtain a wide family of dihedral f-tilings.

2. F-TILINGS BY TRIANGLES (β, γ, δ) AND $(\frac{2\pi}{3}, \frac{\pi}{4}, \frac{\pi}{4})$

We begin by stating the main result of this paper.

Theorem 2.1. *Let $T = (\beta, \gamma, \delta)$ and $T' = (\frac{2\pi}{3}, \frac{\pi}{4}, \frac{\pi}{4})$ be spherical triangles with $\beta = \frac{\pi}{2}$, $\gamma = \frac{\pi}{3}$ and $\delta = \frac{\pi}{4}$. Then $\Omega(T, T') = \{\mathcal{F}_i, 1 \leq i \leq 8\}$, where the \mathcal{F}_i 's are the non-isomorphic f-tilings illustrated in Figure 2.*

The angles around vertices are listed in Figure 3.

Proof. In order to get any dihedral f-tiling $\tau \in \Omega(T, T')$, we find useful to start by considering one of its local configurations, labeling the tiles according to the following procedures:

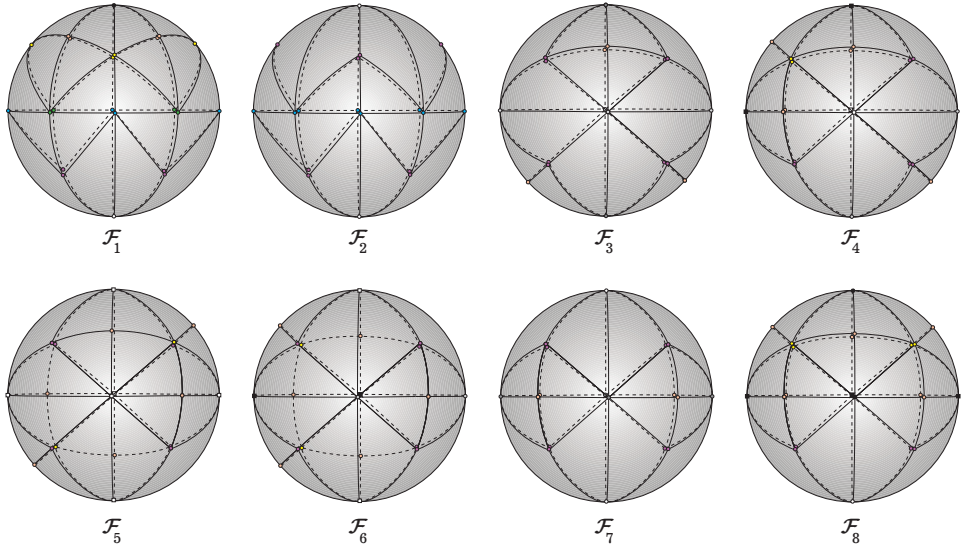


FIGURE 2. Dihedral f-tilings of S^2 with prototiles T and T'

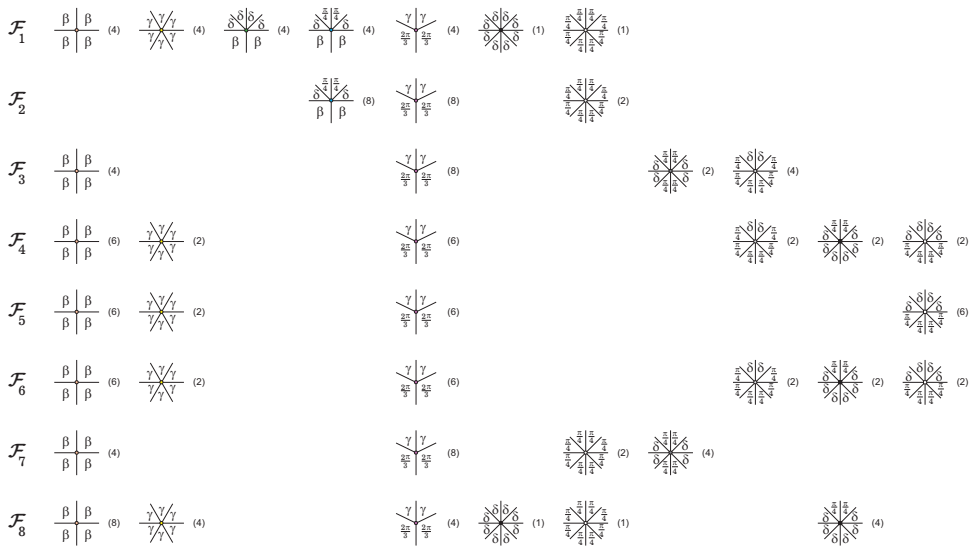


FIGURE 3. Distinct classes of congruent vertices

(i) We begin the configuration of an f-tiling $\tau \in \Omega(T, T')$ with two adjacent triangles both congruent to T' and labeled by 1 and 2 (Figure 4); then we

label with 3 a triangle T , adjacent to T' (observe that there exists such triangle since the f-tiling is dihedral).

- (ii) For $j \geq 4$, the location of tile j can be deduced from the configuration of tiles $1, 2, 3, \dots, j - 1$ and from the hypothesis that the configuration is part of a complete f-tiling (except in the cases indicated).

As both triangles have an identical angle, to simplify the exposition we will consider the angles of T as (β, γ, δ) instead of $(\frac{\pi}{2}, \frac{\pi}{3}, \frac{\pi}{4})$, in order to distinguish whether an angle $\frac{\pi}{4}$ refers to T or T' .

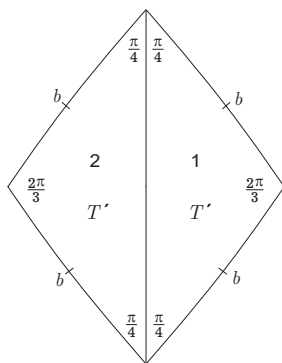


FIGURE 4. Two triangles T' must be adjacent by the larger side

Due to the symmetry of the configuration presented in Figure 4, we will consider the two possible cases of adjacency illustrated in Figure 5.

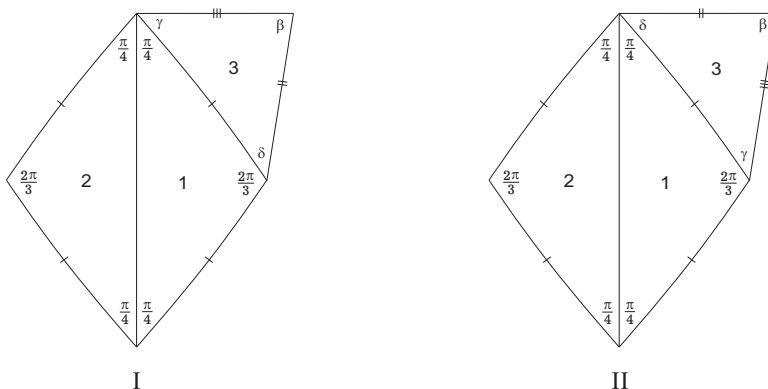


FIGURE 5. Distinct cases of adjacency

1. Consider firstly the case of adjacency I and a vertex surrounded by adjacent angles $\frac{2\pi}{3}$ and δ . Taking into account the available angles, we must have $\frac{2\pi}{3} + \gamma = \pi$

as an alternated angle sum around such a vertex. However, there is no way to satisfy the angle folding relation around this vertex, since $\delta + \rho < \pi$, for all $\rho \in \{\frac{2\pi}{3}, \frac{\pi}{4}, \beta, \gamma, \delta\}$.

2. Now we will consider the second case of adjacency. The vertex surrounded by the cyclic sequence $(\frac{2\pi}{3}, \gamma, \dots)$ must satisfy $\frac{2\pi}{3} + \gamma = \pi$ and the initial local configuration extends to the one illustrated in Figure 6-I. For convenience we may also consider Figure 6-II.

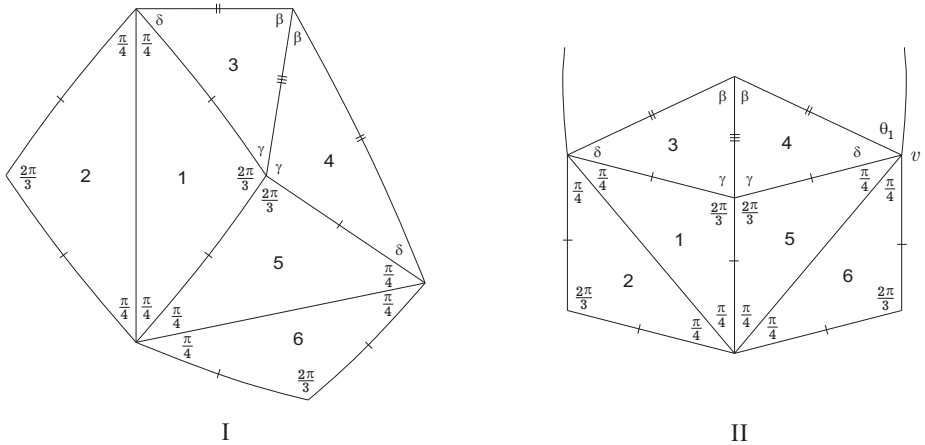


FIGURE 6. Local configurations

With the labeling of Figure 6-II at vertex v we have necessarily

$$\theta_1 = \beta \quad \text{or} \quad \theta_1 = \delta.$$

2.1 Suppose firstly that $\theta_1 = \beta$. It follows that v is a vertex of valency six and the previous configuration gives rise to the one that follows (Figure 7).

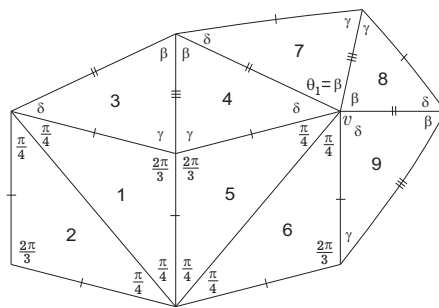


FIGURE 7. Local configuration

The cyclic sequence that surrounds v is $(\frac{\pi}{4}, \frac{\pi}{4}, \delta, \beta, \beta, \delta)$, with $\beta + \delta + \frac{\pi}{4} = \pi$. Now, the planar configuration extends to the one illustrated in Figure 8, where a decision must be made about the angle θ_2 , adjacent to tile 7.

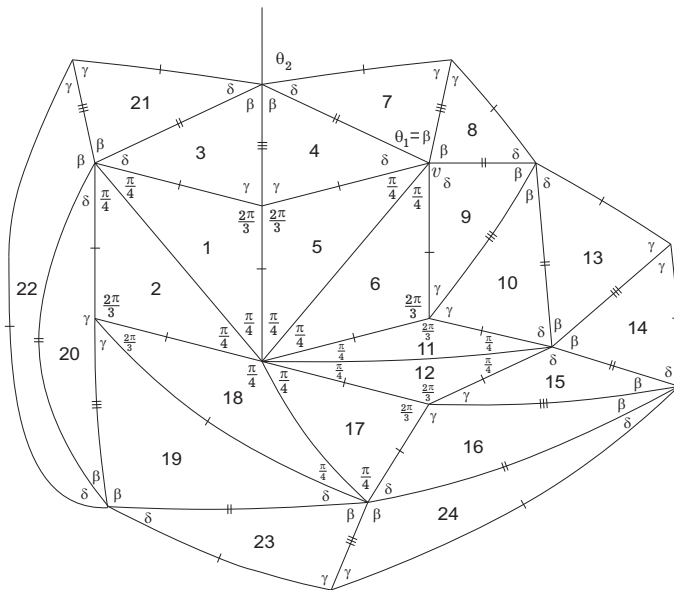


FIGURE 8. Local configuration

Analyzing the edge lengths and the relation between angles, we have

$$\theta_2 = \delta \quad \text{or} \quad \theta_2 = \frac{\pi}{4}.$$

2.1.1 We begin by considering $\theta_2 = \delta$. In this case the last configuration extends in a unique way to close in a complete planar representation (Figure 9). We denote this f-tiling by \mathcal{F}_1 .

A 3D representation is given in Figure 10.

2.1.2 Consider now $\theta_2 = \frac{\pi}{4}$. In this case the local configuration illustrated in Figure 8 extends to give rise to the planar representation illustrated in Figure 11. We denote this f-tiling by \mathcal{F}_2 .

A 3D representation is given in Figure 12.

2.2 We shall consider here that $\theta_1 = \delta$. The local configuration illustrated in Figure 6-II extends as follows (Figure 13).

With the labeling of Figure 13, one has

$$\theta_2 = \frac{\pi}{4} \quad \text{or} \quad \theta_2 = \delta.$$

2.2.1 We begin by considering $\theta_2 = \frac{\pi}{4}$. In this case the last configuration extends to obtain the one in Figure 14-I. Observe that we must choose $\tilde{\theta}_1 = \delta$. In fact if

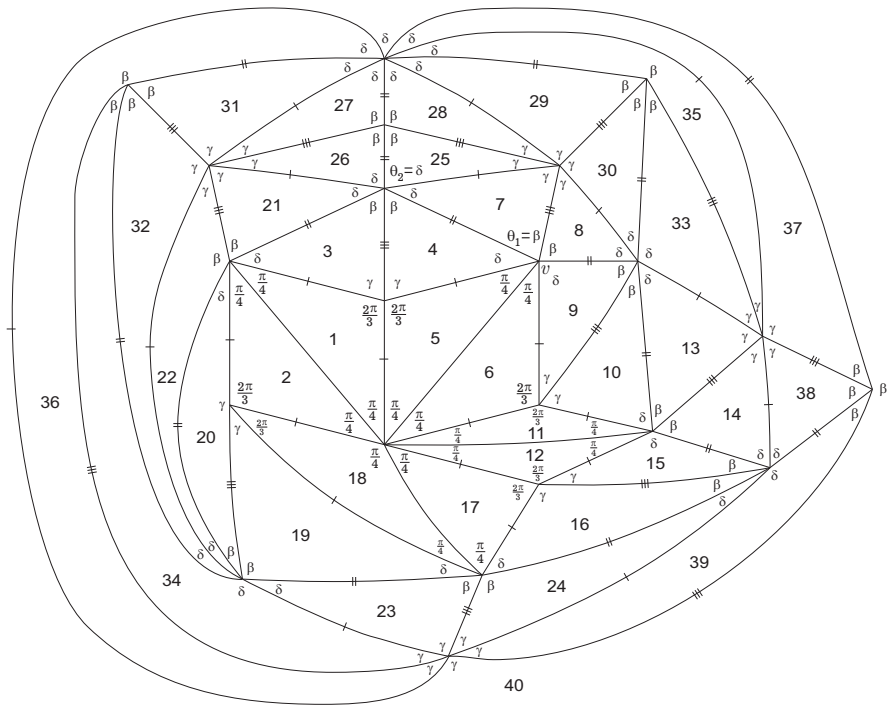


FIGURE 9. Planar representation of \mathcal{F}_1

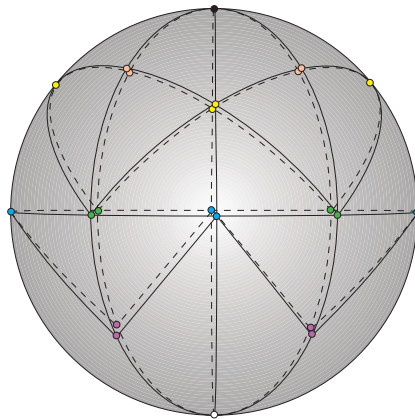


FIGURE 10. 3D representation of \mathcal{F}_1

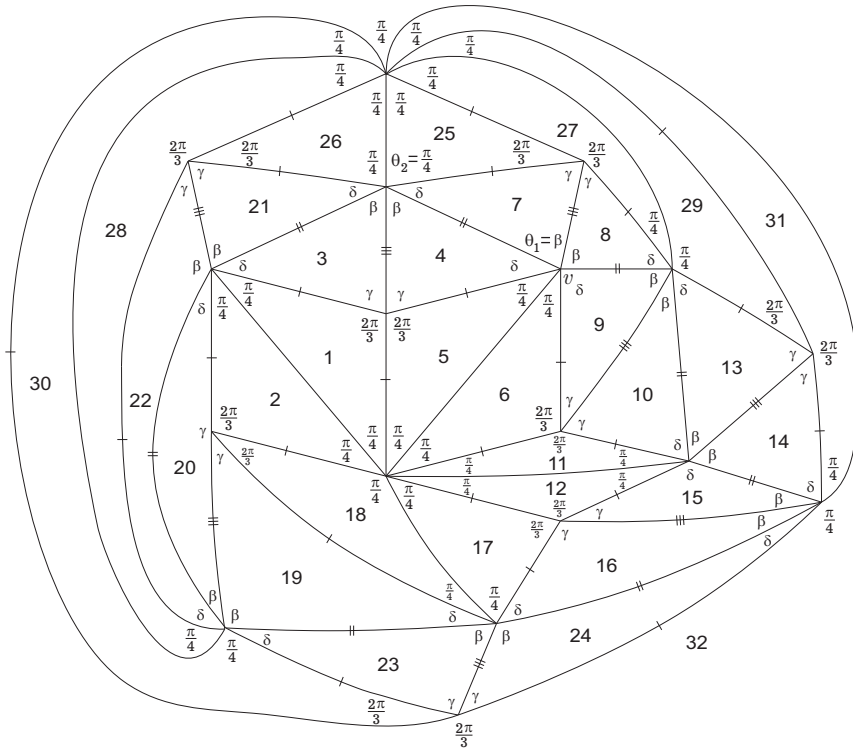


FIGURE 11. Planar representation of \mathcal{F}_2

we consider $\tilde{\theta}_1 = \beta$ then the set of tiles $\{12, 9, 6, 5, 11, 10, 13\}$ leads to the same f-tilings as the ones obtained with tiles $\{1, 2, 3, 4, 5, 6, 7\}$, in which $\theta_1 = \beta$ — a case already studied. Therefore $\tilde{\theta}_1 = \delta$ in what follows; see Figure 14-II.

With the labeling of Figure 14-II, we must have

$$\theta_3 = \frac{\pi}{4} \quad \text{or} \quad \theta_3 = \delta.$$

2.2.1.1 Firstly consider that $\theta_3 = \frac{\pi}{4}$. Then the configuration extends as illustrated in Figure 15. Note that the argument used for $\tilde{\theta}_1$ also applies to $\tilde{\theta}_1$. And so we have also considered $\tilde{\theta}_1 = \delta$.

Once again we must have

$$\theta_4 = \frac{\pi}{4} \quad \text{or} \quad \theta_4 = \delta.$$

2.2.1.1.1 If $\theta_4 = \frac{\pi}{4}$ then we get the planar representation illustrated in Figure 16. We denote this f-tiling by \mathcal{F}_3

A 3D representation is given in Figure 17.

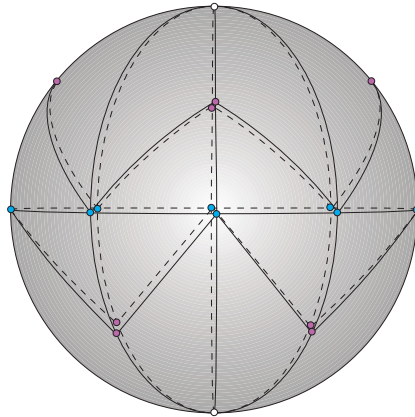


FIGURE 12. 3D representation of \mathcal{F}_2

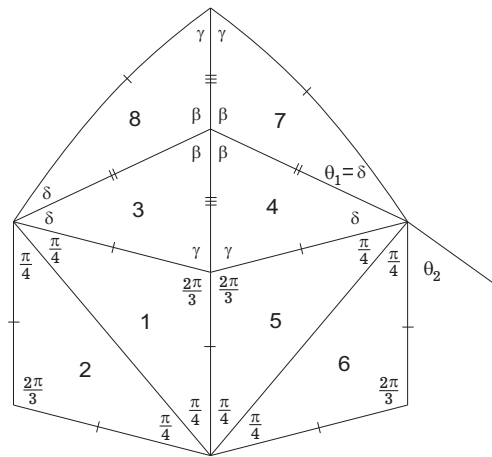


FIGURE 13. Local configuration

2.2.1.1.2 If $\theta_4 = \delta$ then we obtain the planar representation illustrated in Figure 18. We denote this f-tiling by \mathcal{F}_4 .

A 3D representation is given in Figure 19.

2.2.1.2 Now we must consider $\theta_3 = \delta$ (in Figure 14-II). In order to fulfill the angle folding relation everywhere we obtain the configuration below (Figure 20).

Again, we have to distinguish the cases

$$\theta_4 = \frac{\pi}{4} \quad \text{or} \quad \theta_4 = \delta.$$

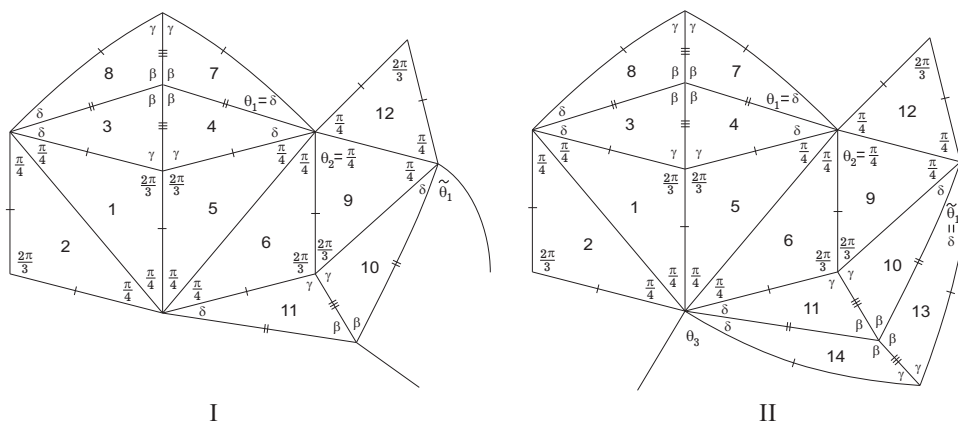


FIGURE 14. Local configurations

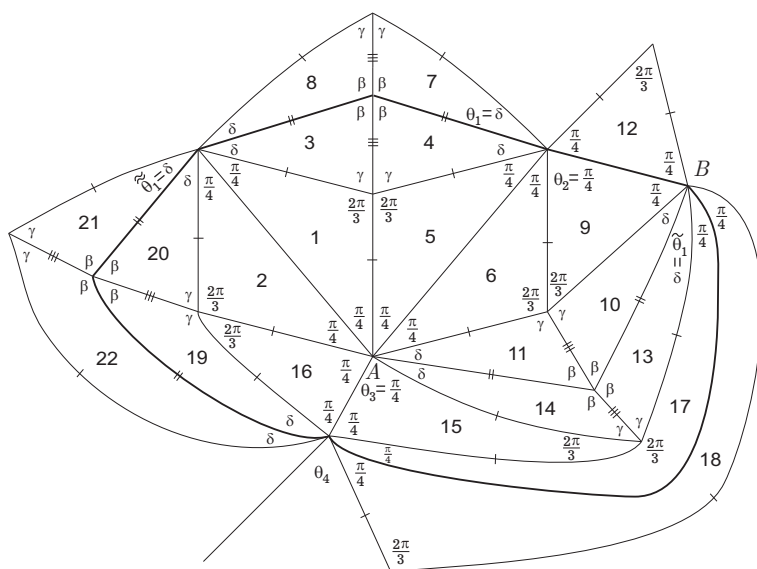


FIGURE 15. Local configuration

2.2.1.2.1 If $\theta_4 = \frac{\pi}{4}$ then we get the planar representation illustrated in Figure 21, whose f-tiling we denote by \mathcal{F}_5 .

A 3D representation is given in Figure 22.

2.2.1.2.2 If $\theta_4 = \delta$ then we obtain the planar representation illustrated in Figure 23. We denote this f-tiling by \mathcal{F}_6 .

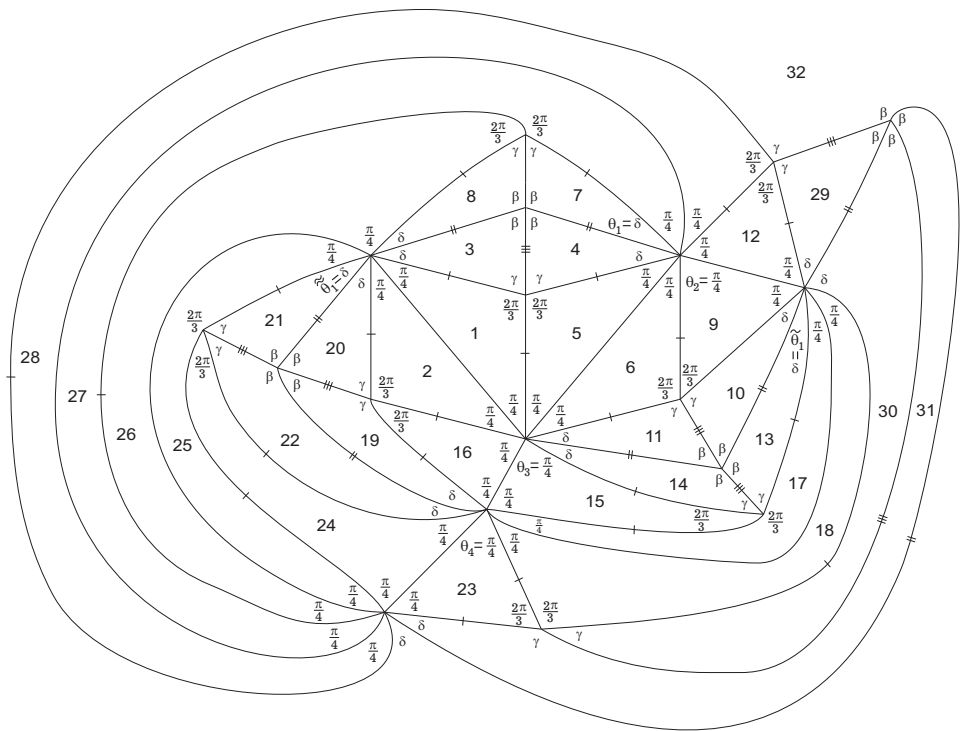


FIGURE 16. Planar representation of \mathcal{F}_3

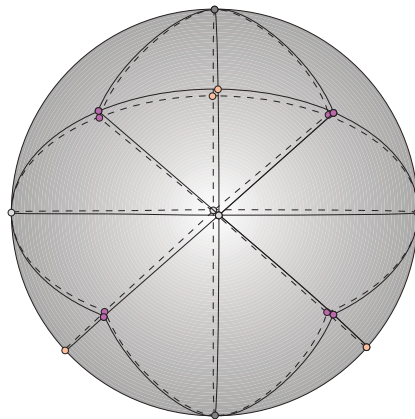


FIGURE 17. 3D representation of \mathcal{F}_3

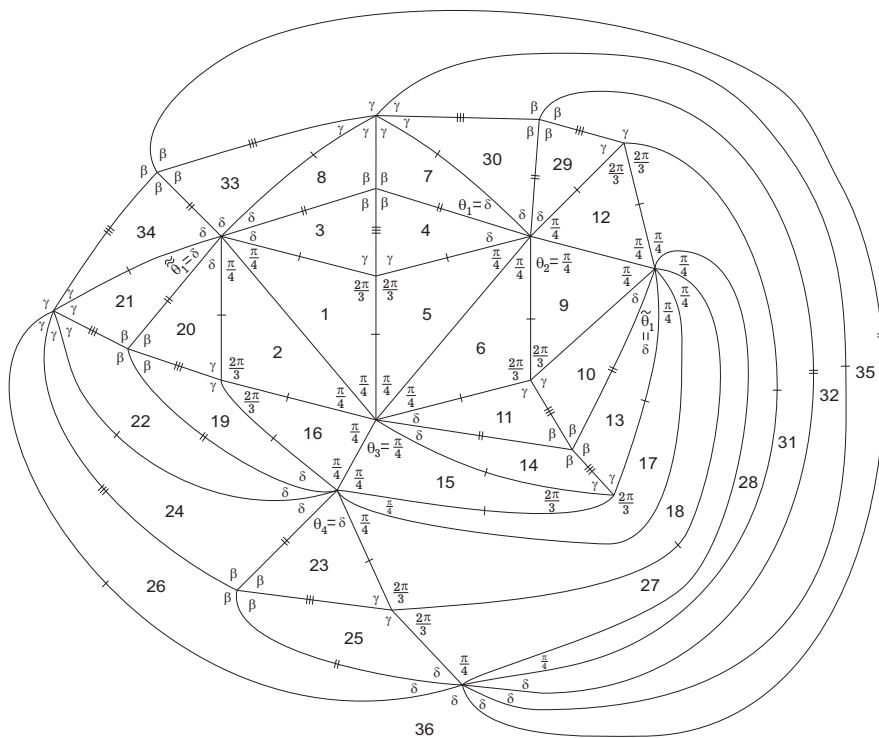


FIGURE 18. Planar representation of \mathcal{F}_4

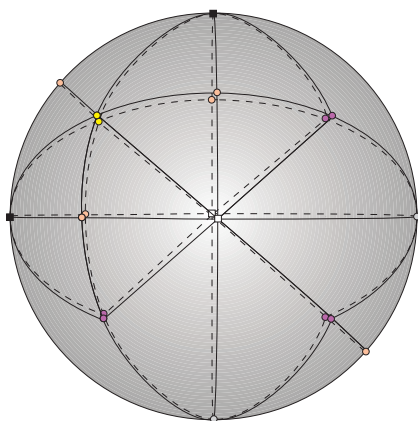


FIGURE 19. 3D representation of \mathcal{F}_4

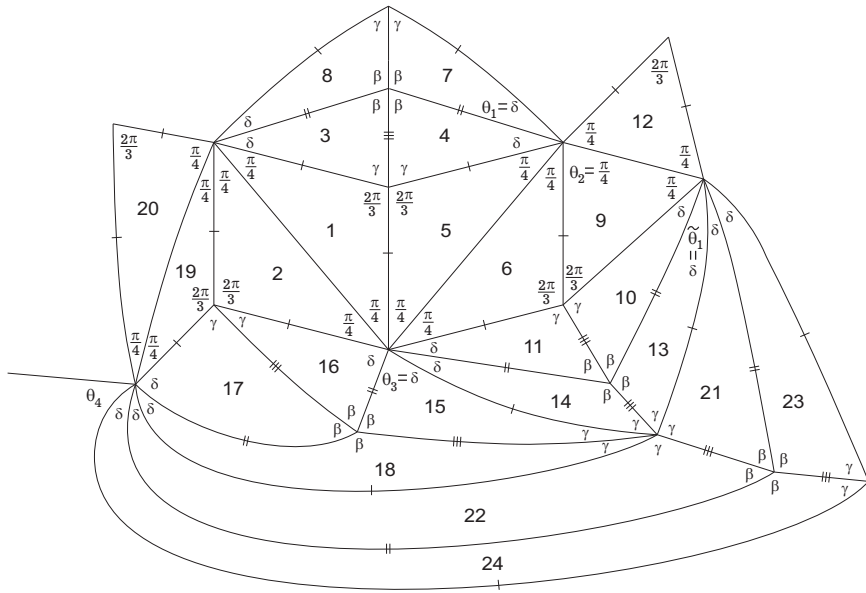


FIGURE 20. Local configuration

A 3D representation is given in Figure 24.

2.2.2 Suppose here that $\theta_2 = \delta$ (see Figure 13). The initial configuration extends now to get the one illustrated in Figure 25.

We have to distinguish two situations:

$$\theta_3 = \delta \quad \text{or} \quad \theta_3 = \frac{\pi}{4}.$$

2.2.2.1 The first hypothesis ($\theta_3 = \delta$) leads us to the following configuration (Figure 26).

The regions inside the dark lines in Figure 26 and Figure 15 are coincident. The same happens with the tiles outside the dark lines (see the position of vertices A and B in both figures). This means that the f-tilings obtained from these two configurations are the same. That is, the choice of $\theta_4 = \frac{\pi}{4}$ and $\theta_4 = \delta$ in Figure 26 leads us to the previous f-tilings, namely \mathcal{F}_3 and \mathcal{F}_4 (obtained in 2.2.1.1.1 and 2.2.1.1.2, respectively).

2.2.2.2 The second hypothesis ($\theta_3 = \frac{\pi}{4}$) leads us to the following configuration (Figure 27).

Now, one has

$$\theta_4 = \frac{\pi}{4} \quad \text{or} \quad \theta_4 = \delta.$$

2.2.2.2.1 If $\theta_4 = \frac{\pi}{4}$ we obtain the planar representation illustrated in Figure 28. We denote this f-tiling by \mathcal{F}_7 .

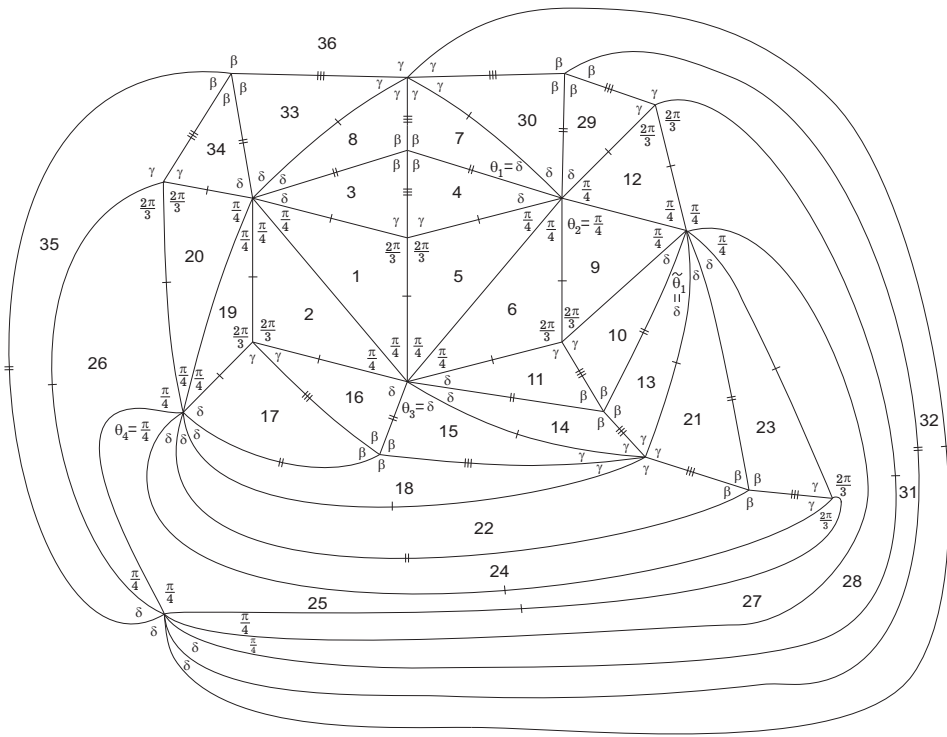


FIGURE 21. Planar representation of \mathcal{F}_5

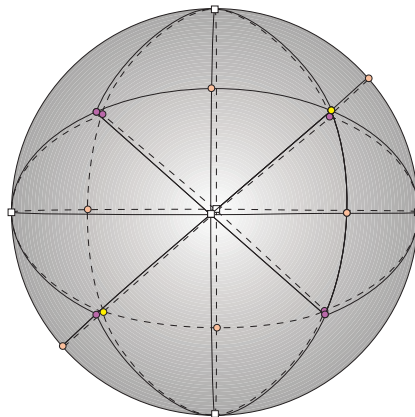


FIGURE 22. 3D representation of \mathcal{F}_5

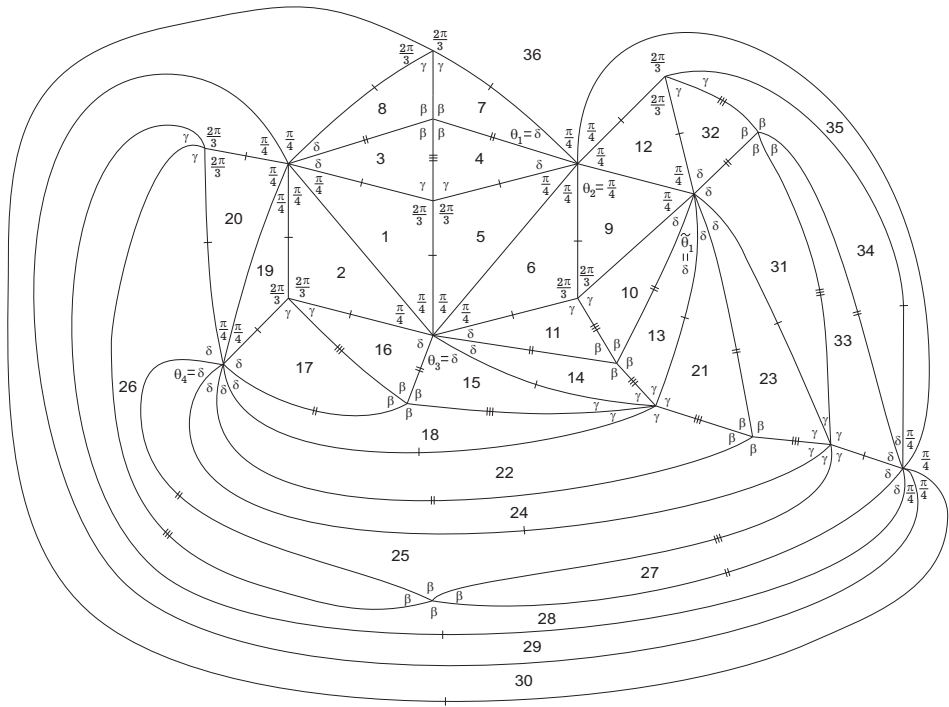


FIGURE 23. Planar representation of \mathcal{F}_6

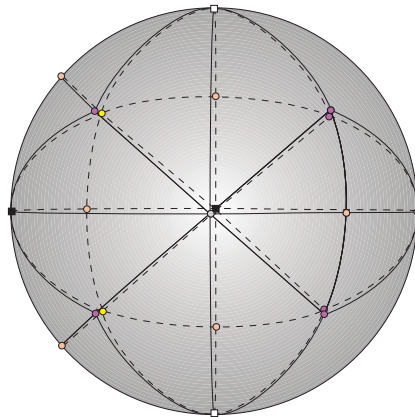


FIGURE 24. 3D representation of \mathcal{F}_6

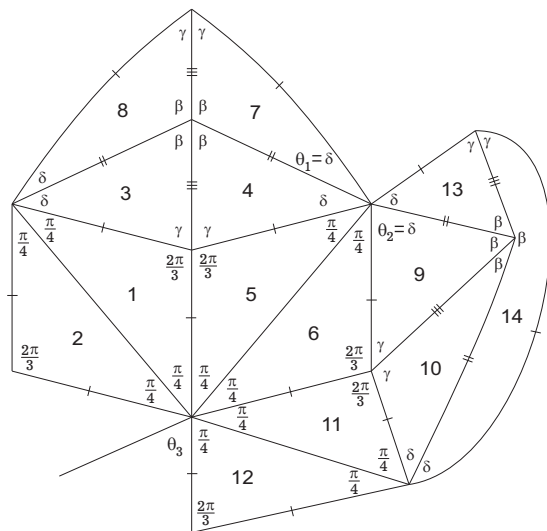


FIGURE 25. Local configuration

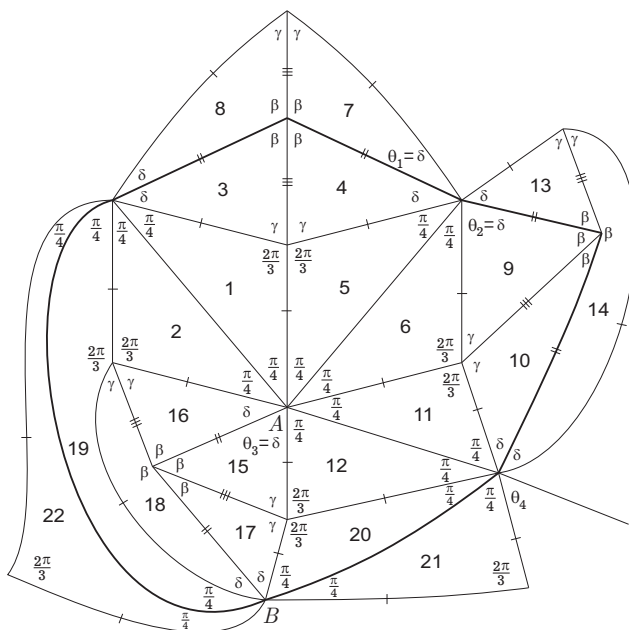


FIGURE 26. Local configuration

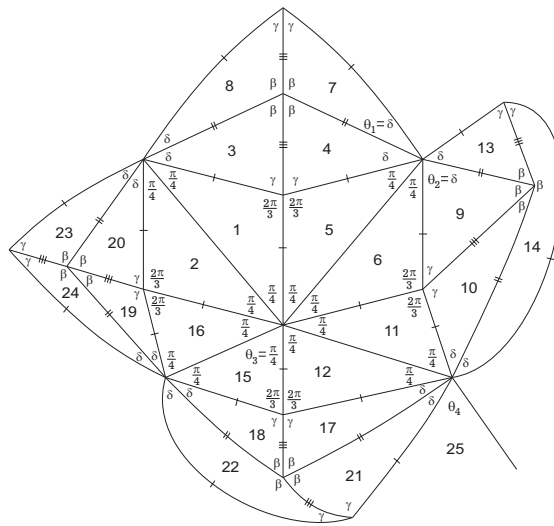


FIGURE 27. Local configuration

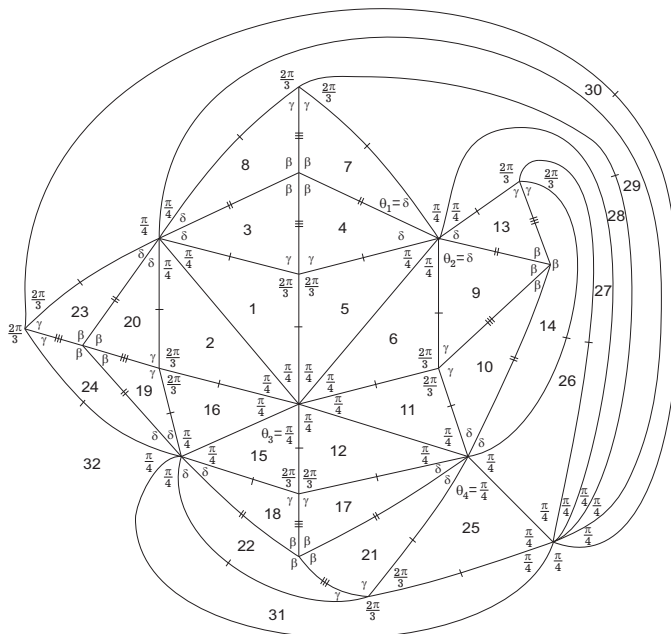


FIGURE 28. Planar representation of \mathcal{F}_7

A 3D representation is given in Figure 29.

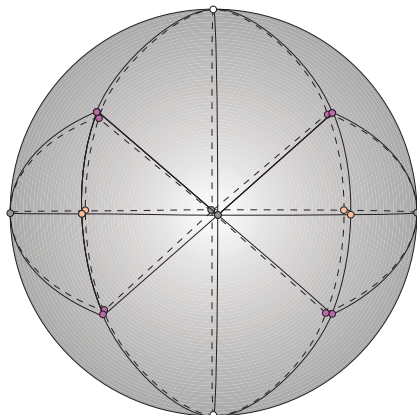


FIGURE 29. 3D representation of \mathcal{F}_7

2.2.2.2.2 Finally, if $\theta_4 = \delta$ we obtain the planar representation illustrated in Figure 30. We denote this f-tiling by \mathcal{F}_8 .

A 3D representation is given in Figure 31.

□

3. SUMMARY

In Table 1 is shown a list of all spherical dihedral f-tilings whose prototiles are the spherical triangles T and T' of internal angles $\beta = \frac{\pi}{2}$, $\gamma = \frac{\pi}{3}$, $\delta = \frac{\pi}{4}$ and $\frac{2\pi}{3}$, $\frac{\pi}{4}$, $\frac{\pi}{4}$, respectively. Our notation is as follows:

- $|V|$ is the number of distinct classes of congruent vertices.
- N_1 and N_2 are, respectively, the number of triangles congruent to T and T' used in the dihedral f-tilings; note that $N_1 + 2N_2 = 48$.
- $G(\tau)$ is the symmetry group of each tiling $\tau \in \Omega(T, T')$; C_n is the cyclic group of order n ; by D_n we mean the dihedral group of order $2n$.

Concerning the combinatorial structure of each tiling obtained before, we follow the notation used in previous papers.

Any symmetry of \mathcal{F}_1 fixes $N = (0, 0, 1)$ (and consequently $S = -N$). It is generated, for instance, by the rotation $R_{\frac{z}{2}}$ (around the z axis) and the reflection ρ^{yz} (on the coordinate plane yoz), giving rise to a group isomorphic to D_4 (the dihedral group of order 8). The same applies to \mathcal{F}_8 .

The f-tilings \mathcal{F}_2 and \mathcal{F}_7 have only two vertices surrounded by angles $\frac{\pi}{4}$, say the north and south poles. The symmetries of \mathcal{F}_2 and \mathcal{F}_7 that fix the north pole are generated by a reflection and by the rotation through an angle $\frac{\pi}{2}$ around the zz axis, $R_{\frac{z}{2}}$, giving rise to a subgroup isomorphic to D_4 . Now, the map $\rho^{xy} \circ R_{\frac{z}{4}}$ is also a symmetry of \mathcal{F}_2 , and so it follows that the symmetry group of \mathcal{F}_2 is isomorphic

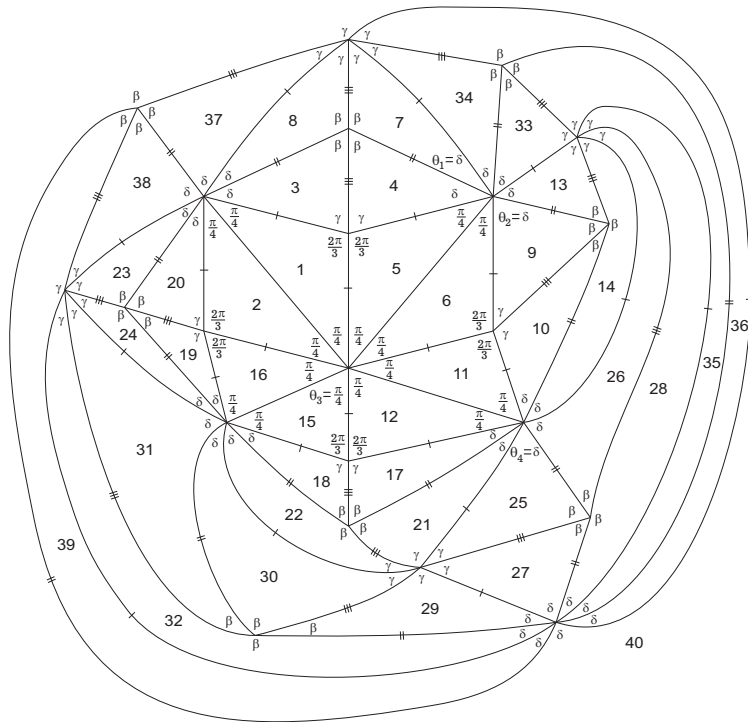


FIGURE 30. Planar representation of \mathcal{F}_8

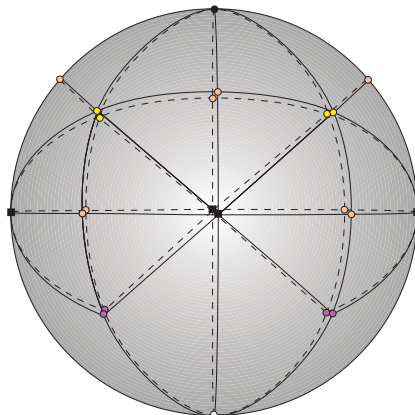


FIGURE 31. 3D representation of \mathcal{F}_8

f-tiling	$ V $	N_1	N_2	$G(\tau)$
\mathcal{F}_1	7	32	8	D_4
\mathcal{F}_2	3	16	16	D_8
\mathcal{F}_3	4	16	16	D_4
\mathcal{F}_4	6	24	12	$D_2 = C_2 \times C_2$
\mathcal{F}_5	4	24	12	D_6
\mathcal{F}_6	6	24	12	C_2
\mathcal{F}_7	4	16	16	$C_2 \times D_4$
\mathcal{F}_8	6	32	8	D_4

TABLE 1. Combinatorial structure of the dihedral f-tilings of S^2 by triangles $(\frac{\pi}{2}, \frac{\pi}{3}, \frac{\pi}{4})$ and $(\frac{2\pi}{3}, \frac{\pi}{4}, \frac{\pi}{4})$

to D_8 generated by $\rho^{xy} \circ R_{\frac{\pi}{4}}^z$ and ρ^{yz} , for instance. Concerning \mathcal{F}_7 , we have that ρ^{xy} commutes the north and south poles and so $G(\mathcal{F}_7)$ is isomorphic to $C_2 \times D_4$.

Any symmetry of \mathcal{F}_3 fixes $N = (0, 0, 1)$ (and consequently $S = -N$) or maps N into S (and consequently S into N). The symmetries that fix N are generated, for instance, by the rotation $R_{\frac{\pi}{2}}^z$ (around the z axis) and the reflection ρ^{yz} (on the coordinate plane $yo z$), giving rise to a subgroup of \mathcal{F}_3 isomorphic to $D_2 = C_2 \times C_2$ (the dihedral group of order 4). Now, the map $\phi = R_{\frac{\pi}{2}}^z \circ \rho^{xy}$ is a symmetry of \mathcal{F}_3 that permutes N and S allowing us to get all the symmetries that map N into S . One has $\phi^3 \circ \rho^{yz} = \rho^{yz} \circ \phi$ and ϕ has order 4. It follows that ϕ and ρ^{yz} generate $G(\mathcal{F}_3)$. And so it is isomorphic to D_4 .

The study of the symmetry group of the remaining f-tilings is similar.


REFERENCES

[1] C. P. Avelino and A. F. Santos, S^2 coverings by isosceles and scalene triangles—adjacency case I, *Ars Math. Contemp.* **16** (2019), no. 2, 419–443. MR 3963216.
 [2] A. M. R. Azevédo Breda, A class of tilings of S^2 , *Geom. Dedicata* **44** (1992), no. 3, 241–253. MR 1193117.
 [3] A. M. d’Azevedo Breda, P. S. Ribeiro and A. F. Santos, Dihedral f-tilings of the sphere by equilateral and scalene triangles. III, *Electron. J. Combin.* **15** (2008), no. 1, Research Paper 147, 34 pp. MR 2465771.
 [4] A. M. d’Azevedo Breda, P. S. Ribeiro and A. F. Santos, A class of spherical dihedral f-tilings, *European J. Combin.* **30** (2009), no. 1, 119–132. MR 2460222.
 [5] R. J. MacG. Dawson, Tilings of the sphere with isosceles triangles, *Discrete Comput. Geom.* **30** (2003), no. 3, 467–487. MR 2002969.
 [6] R. J. MacG. Dawson and B. Doyle, Tilings of the sphere with right triangles. I. The asymptotically right families, *Electron. J. Combin.* **13** (2006), no. 1, Research Paper 48, 31 pp. MR 2223523.

- [7] R. J. MacG. Dawson and B. Doyle, Tilings of the sphere with right triangles. II. The $(1, 3, 2), (0, 2, n)$ subfamily, *Electron. J. Combin.* **13** (2006), no. 1, Research Paper 49, 22 pp. MR 2223524.
- [8] S. A. Robertson, Isometric folding of Riemannian manifolds, *Proc. Roy. Soc. Edinburgh Sect. A* **79** (1977/78), no. 3-4, 275–284. MR 0487893.
- [9] Y. Ueno and Y. Agaoka, Classification of tilings of the 2-dimensional sphere by congruent triangles, *Hiroshima Math. J.* **32** (2002), no. 3, 463–540. MR 1954054.

Catarina P. Avelino

Department of Mathematics, UTAD, 5001-801 Vila Real, Portugal
cavelino@utad.pt

Altino F. Santos 

Department of Mathematics, UTAD, 5001-801 Vila Real, Portugal
afolgado@utad.pt

Received: April 29, 2019

Accepted: October 2, 2019